Research Article

For reprint orders, please contact: reprints@futuremedicine.com

Nanomedicine

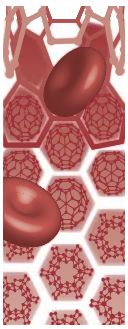

Polymeric micelles for *MCL-1* gene silencing in breast tumors following systemic administration

Aim: To develop delivery systems for efficient siRNA delivery to breast cancer. **Methods:** Poly(ethylene oxide)-*block*-poly(ε-caprolactone-*grafted*-spermine) (PEO-*b*-P(CL-*g*-SP)) micelles were modified with cholesterol group in their core and with RGD4C peptide on their shell. Transfection efficiency of complexed MCL-1 siRNA in MDA-MB-435 was investigated, *in vitro* and *in vivo* following intratumoral and intravenous injection. **Results:** Cholesteryl modification of the core significantly increased the transfection efficiency of PEO-*b*-P(CL-*g*-SP)-complexed siRNA, *in vitro*, but not following intratumoral or intravenous administration, *in vivo*. Instead, RGD4C modification of the micellar shell enhanced transfection efficiency of complexed MCL-1 siRNA in tumor upon intravenous administration. **Conclusion:** RGD4C-PEO-*b*-P(CL-*g*-SP) micelles, without or with cholesterol modification, can provide efficient delivery of siRNA to breast tumors following systemic administration.

First draft submitted: 24 April 2016; Accepted for publication: 5 July 2016; Published online: 16 August 2016

Keywords: cancer • cholesterol • MCL-1 • MDA-MB-435 • PEO-*b*-PCL • polymeric micelles • RGD4C • siRNA delivery • spermine

Shyam M Garg[‡,1], Arash Falamarzian[‡,1], Mohammad Reza Vakili[1], Hamidreza M Aliabadi[3], Hasan Uludağ[1,2] & Afsaneh Lavasanifar*[,‡,,1,2]

[1]Faculty of Pharmacy & Pharmaceutical Sciences, University of Alberta, Edmonton, AB T6G 2E1, Canada

[2]Department of Chemical & Materials Engineering, Faculty of Engineering, University of Alberta, Edmonton, AB, T6G 2V4, Canada

[3]Department of Biomedical & Pharmaceutical Sciences, School of Pharmacy, Chapman University, Irvine, CA 92618, USA

*Author for correspondence:
Tel.: +1 780 492 2742
Fax: +1 780 4921 217
afsaneh@ualberta.ca

[‡]Authors contributed equally

Despite great promise of gene-silencing agents such as siRNA, translation of this approach to clinical practice particularly following systemic administration has been challenging. This is mostly due to the instability of siRNA and other gene-silencing agents in plasma, rapid renal excretion, poor distribution to target tissue and inadequate access to their molecular targets within the cells of interest. Several delivery systems developed to address these issues, are mostly successful in siRNA delivery *in vitro* or following localized *in vivo* administration [1–3]. Success in the targeted delivery of siRNA, particularly to tumors, following systemic administration has been limited mostly due to the nonspecific toxicity imposed by the siRNA carrier, uptake by the reticuloendothelial system, insufficient stability in blood, and/or insufficient delivery to tumor tissue and/or cancer cells [4].

Amphiphilic block copolymers with poly(ethylene oxide) (PEO) as the shell-forming block and polyesters like poly(ε-caprolactone) (PCL) [5,6], poly(lactide) [7] or poly(lactide-*co*-glycolide) [8,9] as the core-forming block have shown tremendous potential in drug delivery [10,11]. This is due to the biocompatibility of PEO and polyesters as well as the biodegradability of polyesters, making them safe for human administration [12]. Our research group has previously reported the development of a biodegradable and biocompatible siRNA delivery system based on self-associating PEO-*b*-PCL block copolymers bearing polycationic spermine (SP) on the α-carbons of ε-caprolactone of the PCL block. The poly(ethylene oxide)-*block*-poly(ε-caprolactone-*grafted*-spermine) (PEO-*b*-P[CL-*g*-SP]) micelles were able to protect siRNA from degradation by serum nucleases, internalize siRNA into cancer

Future Medicine part of fsg

cells and effectively downregulate *MDR-1* through delivery of its siRNA leading to significant decrease in the expression of P-glycoprotein in multidrug-resistant (MDR) MDA-MB-435/MDR cells [13]. Further modification of PEO-*b*-P(CL-*g*-SP) micellar shell with cancer-targeting and cell-penetrating peptides, that is, RGD4C and TAT, respectively, increased the transfection efficiency of the MDR-1 siRNA, *in vitro* [14]. Systemic administration of RGD4C-modified PEO-*b*-P(CL-*g*-SP) was also shown to enhance the localization of siRNA in tumor in an MDA-MB-435 xenograft model pointing to the potential of this nanocarrier for siRNA delivery following systemic administration [15]. The aim of this study was to assess this potential for PEO-*b*-P(CL-*g*-SP) micelles and their core/shell-modified counterparts.

Hydrophobic or lipid modification of polymeric complexes has been shown to increase the efficacy of nonviral gene delivery vectors through enhancing their interaction with plasma membrane facilitating cell uptake [16,17]. For instance, cholesteryl modification of linear and branched polyethyleneimine (PEI) has shown to significantly enhance cellular uptake and transfection efficiency of linear and branched PEI complexes of pDNA and siRNA in cancer cells [18–20]. In another study, Wang *et. al.* showed efficient transfection of Bcl-2 siRNA in MDA-MB-231 breast cancer cells by core/shell nanoparticles containing cholesteryl-modified amine groups [21], although the specific role of cholesteryl group could not be verified due to lack of results for control of unmodified nanoparticles. In light of positive effect of cholesteryl substituents on polycations for the transfection efficiency of siRNA, in the current study, we modified the SP groups of PEO-*b*-P(CL-*g*-SP) micelles with cholesterol and studied the effect of this approach in plain and/or RGD4C-modified micelles on siRNA delivery and silencing of *MCL-1* in human MDA-MB-435 models, *in vitro* and *in vivo*.

MCL-1 is an antiapoptotic member of the Bcl-2 family of proteins, which maintains survival of cells by inhibiting cytochrome c release *via* binding and sequestering proapoptotic Bcl-2 proteins [3,22–24]. Upregulation of MCL-1 is implicated in cancer survival in a variety of human hematological [23,25] as well as solid cancers [26,27]. Downregulation of MCL-1, on the other hand, is implicated in the induction of apoptosis [28]. Many synthetic and natural chemicals were shown to inhibit MCL-1 expression either at pre- or post-transcription stages. This includes cyclin-dependent kinase inhibitors such as flavopiridol [29], tyrosine kinase inhibitors such as sorafenib [27] and STAT3 inhibitors such as resveratrol [30]. However, these compounds lack specificity for MCL-1 and affect multiple molecular targets [28]. Specific inhibitors of MCL-1 are divided into two classes of compounds: BH3 mimetics and gene-silencing treatments. BH3 mimetics like Obatoclax and Bim_S2A can antagonize the interaction of MCL-1 with proapoptotic proteins [26,28,31,32]. However, many of these compounds have shown to cause nonspecific cytotoxicity by damaging mitochondria [26]. An alternative and more specific approach is downregulation of MCL-1 expression through gene silencing *via* antisense oligonucleotides [33] or siRNA. Knockdown of *MCL-1* using siRNA in resistant melanoma cells is shown to sensitize these cells toward Fas-mediated apoptosis [34]. Modugno *et. al.* tested 44 solid cancer cell lines with MCL-1 siRNA and found downregulation of MCL-1 expression to induce apoptosis in 30% of the tested cell lines [26]. In MDA-MB-435 cells, *MCL-1* silencing using PEI-linoleic acid (PEI-LA) complexed with MCL-1 siRNA was able to decrease the MCL-1 mRNA expression by approximately 80% and also reduced cell viability by up to approximately 50%, *in vitro*. *In vivo* studies in MDA-MB-435 xenografts showed an approximately 35% decrease in *MCL-1* mRNA expression and delayed tumor growth after intratumoral injections with PEI-LA/MCL-1 siRNA complexes [35]. Collectively, this experience indicated MCL-1 to be an effective target for siRNA delivery.

Materials & methods

Materials

Branched PEI with a molar mass of 25 kDa (PEI25K), 3,3-Diethoxy-1-propanol, naphthalene, potassium (in mineral oil), methoxy polyethylene oxide (M_w 5000 Da), ethylene oxide, N,N-dicyclohexyl carbodiimide, N-hydroxysuccinimide, pyrene, SP, N,N-dimethyldipropylenetriamine (DP), cholesteryl chloroformate, anhydrous DMF, Hank's Balanced Salt Solution (HBSS) and 3-(4,5-Dimethylthiazol-2-yl)-2,5-diphenyltetrazolium bromide (MTT) were obtained from Sigma (MO, USA). α-Benzyl carboxylate-ε-caprolactone monomer was synthesized by Alberta Research Chemicals, Inc. (Edmonton, Alberta, Canada) according to a previously published procedure [36]. Stannous octoate was purchased from MP Biomedicals, Inc. (Eschwege, Germany). Acetone, THF and DMF were obtained from Caledon Laboratories Ltd (ON, Canada). RGD4C (KACDCRGDCFCG, MW 1273.9) was purchased from Anaspec, Inc. (CA, USA). All other chemicals were of reagent grade. Cell culture media RPMI 1640, penicillin-streptomycin-glutamine, fetal bovine serum, HEPES buffer solution (1 M) and trypsin/EDTA were purchased from GIBCO, Invitrogen Corp. (CA, USA). The scrambled siRNA used as control and Silencer® FAM™ Labeled Negative siRNA were supplied from Ambion (catalog num-

bers: AM4636 and AM4620). The Silencer siRNAs against MCL-1 were purchased from Qiagen (Hilden, Germany; catalog number: SI02781205, sequence: CGCCGAAUUCAUUAAUUUATT).

Cell lines

The wild-type MDA-MB-435 cells were originally obtained as a gift from the laboratory of Dr Robert Clark (Georgetown University, WA, USA). MDA-MB-435 cells were cultured in RPMI 1640 media supplemented with 10% fetal bovine serum, 100 U/ml penicillin and 100 mg/ml streptomycin in 37°C and 5% CO_2. Cell cultures were considered confluent when a monolayer of cells covered >80% of the flask surface. To propagate the cells, a monolayer was washed with sterile PBS, and subsequently incubated with 0.25% trypsin/EDTA for 3 min at 37°C. The suspended cells were centrifuged at 500 × *g* for 5 min, and were resuspended in the medium after removal of the supernatant. The suspended cells were either subcultured at 10% of the original count or seeded in multiwell plates for testing.

Synthesis of cholesteryl-substituted PEO-*b*-P(CL-*g*-SP) block copolymers

Methoxy-poly(ethylene oxide)-*b*-poly(ε-caprolactone-*g*-N-(spermine)-cholesteryl carboxylate) (PEO-*b*-P[CL-*g*-SP-Chol]) was prepared in four steps. In the first step, PEO-*b*-poly(α-benzyl carboxylate-ε-caprolactone) was synthesized by ring-opening polymerization of α-benzyl carboxylate-ε-caprolactone using methoxy-PEO as initiator and stannous octoate as catalyst [36]. In the second step, PEO-b-poly(α-benzyl carboxylate-ε-caprolactone) was reduced to PEO-*b*-poly(α-carboxyl-ε-caprolactone) (PEO-*b*-PCCL) using a constant stream of hydrogen gas to obtain a fully reduced polymer [37]. In the third step, SP was conjugated to PEO-*b*-PCCL forming methoxy-poly(ethylene oxide)-*block*-poly(α-carboxylate-ε-caprolactone-*g*-N-[spermine]) (PEO-*b*-P[CL-*g*-SP]) according to a previously published procedure with slight modification [13]. Briefly, PEO-*b*-PCCL (200 mg, ~0.01 mmol) was dissolved in 10 ml of dry THF. After addition of N,N-dicyclohexyl carbodiimide and N-hydroxysuccinimide in THF, the solution was stirred for 3 h until a precipitate was formed. The precipitate was removed by filtration. THF was removed under vacuum. The remaining solid product was dissolved in DMF. SP was dissolved in DMF and added dropwise to the polymer solution. The reaction proceeded for another 24 h under stirring at room temperature. The resulting solution was centrifuged to remove the precipitate, and the resulting solution was then dialyzed (molecular weight cut-off of 3500 Da) extensively against DMF (24 h) and then water (7 h). The polymer solution was then freeze-dried for further use. After purification, the synthesis of PEO-*b*-P(CL-*g*-SP) was confirmed by ^{1}H NMR (Bruker Avance III spectrometer, Bruker BioSpin Corporation, MA, USA). The SP substitution level of the synthesized copolymer was estimated based on peak intensity ratio of the methylene protons from polyamine (-CH_2-NH-) and PEO (-CH_2CH_2O-). The degree of polymerization was estimated based on peak intensity ratio of proton from PCL (-OCH_2- proton, δ = 4.1 ppm) to the intensity of specific peak in PEO ([-CH_2CH_2O-] proton, δ = 3.65 ppm).

PEO-*b*-P(CL-*g*-SP-Chol) was synthesized by attaching pendant cholesteryl groups to the polyamine section of PEO-*b*-P(CL-*g*-SP) (Figure 1). Briefly, a solution of 0.3 g of PEO-*b*-P(CL-*g*-SP) in 6 ml dried DMF was placed in a round bottom flask under argon atmosphere. This flask was cooled down to 0°C by an ice-water bath. A solution of cholesteryl chloroformate (0.074 g) in 6 ml of dry DMF was added dropwise to previous solution over a period of 45 min. The reaction was left for 24 h at room temperature under argon atmosphere. Finally, the resulting solution was poured into a large amount of ether to precipitate the product. The separated solid product was completely washed by ether and dried under vacuum. The degree of polymerization of PCL backbone after reaction with cholesteryl chloroformate was estimated as described for PEO-*b*-P(CL-*g*-SP). Cholesteryl substitution level was estimated by comparing the peak intensities of (-CH_3 proton, δ = 0.9 ppm) cholesteryl moiety to the intensity of specific peak in PEO ((-CH_2CH_2O-) proton, δ = 3.65 ppm).

Conjugation of RGD4C to polymeric micelles

For *in vivo* studies, acetal-PEO-*b*-PCCL was synthesized according to a previously reported method [38]. DP was then conjugated to acetal-PEO-*b*-PCCL as reported before [13] to produce acetal-poly(ethylene oxide)-*block*-poly[α-carboxylate-(ε-caprolactone)-*graft*-(N,N-dimethyldipropylenetriamine)] (acetal-PEO-*b*-P[CL-*g*-DP]). RGD4C attachment to acetal-PEO-*b*-P(CL-*g*-DP) was then carried out according to a previously reported method [15,39]. RGD4C was conjugated to the micelles at an RGD4C:polymer molar ratio of 1:5. The conjugation efficiency of RGD4C to polymeric micelles was determined by a reverse gradient HPLC method as described previously [15,39]. The resulting polymer solution was dialyzed against distilled water and lyophilized.

Assembly of block copolymers & characterization of self-assembled structures

PEO-*b*-P(CL-*g*-SP) and PEO-*b*-P(CL-*g*-SP-Chol) micelles were prepared simply by dissolving 4 mg

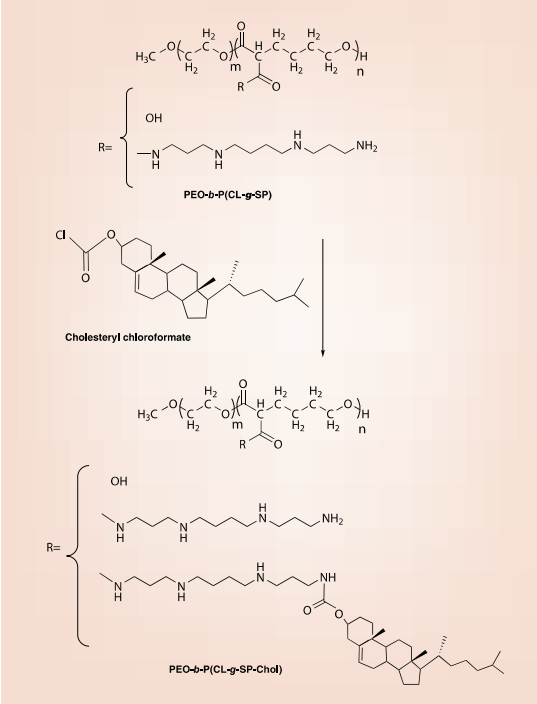

Figure 1. Scheme for the synthesis of poly(ethylene oxide)-*b*-poly(ε-caprolactone-*g*-N-(spermine)-cholesteryl carboxylate).

of block copolymer in doubly distilled water (1 ml) under moderate stirring at 25°C. Average diameter (Z-average) and size distribution of prepared micelles were estimated by dynamic light scattering using a commercial Zetasizer nano ZS (Malvern Instruments, Worcestershire, UK) at a polymer concentration of 2 mg/ml in deionized water at 25°C. Average ζ-potential of prepared particles was estimated using the same instrument by dissolving 2 mg of block copolymer in HEPES buffer (1 ml) under moderate stirring at 25°C.

Morphology of the self-assembled structures was investigated by transmission electron microscopy (TEM). Briefly, an aqueous droplet of micellar solution (10 µl) with a polymer concentration of 1.5 mg/ml was placed on a copper-coated grid. The grid was held horizontally for 1 min to allow the colloidal aggregates to settle, after which, the excess fluid was removed by filter paper. A drop of 2% solution of phosphotungstic acid in PBS (pH 7) was then added to provide the negative stain. After 20 s, the excess fluid was removed by filter paper. The samples were then air-dried and loaded into a Morgagni TEM (Field Emission, Inc., OR, USA) with Gatan digital camera (Gatan, CA, USA). Images were obtained at a magnification of 140,000X at 75 kV.

A change in the fluorescence excitation spectra of pyrene in the presence of varied concentrations of different block copolymers was used to measure their critical micellar concentration (CMC) according to a previously published procedure [40]. The excitation spectrum of pyrene for each sample was obtained at room temperature using a Cary Eclipse fluorescence spectrophotometer (Agilent Technologies, VIC, Australia). Emission wavelength and excitation/emission slit were set at 390 and 5 nm, respectively. The intensity ratio of peaks at 339 nm to those at 334 nm was plotted against the logarithm of copolymer concentration. The CMC was measured from a sharp rise in intensity ratios (I_{339}/I_{334}) at the onset of micellization.

Determination of siRNA binding by SYBR Green dye exclusion assay

The ability of the polymers to bind siRNA was assessed by the SYBR Green II binding assay [41]. Briefly, complexes were prepared by mixing 8 µl of 0.1 M HEPES buffer (pH 6.5) with 4 µl of scrambled siRNA (containing 0.5 µg siRNA) and 8 µl of serially-diluted concentrations of polymeric micellar solutions (containing polymers ranging from 0.5 to 64 µg). After 30 min of incubation at 37°C, 200 µl of the SYBR Green II solution was added to the complexes and the fluorescence of the samples was measured in a 96-well plate (λ_{ex}: 485 nm, λ_{em}: 527 nm) to quantify the amount of free siRNA. The binding curves were generated by plotting the percentage of siRNA bound to the polymer versus polymer:siRNA weight/weight (w/w) ratios. The binding for each polymer was tested at least in two independent experiments.

siRNA release by polyanion competition

As a measure of complex stability, the ability of micelles to release siRNA after challenge with the competing polyanionic heparin was determined. Micelles were prepared at polymer:siRNA ratio of 32:1 (w/w) to ensure complete binding of siRNA by polymers. After incubation of the mixtures for 30 min at 37°C, the resulting complexes were incubated with 0.78, 1.52, 3.04, 6.08, 12.48 and 24.32 µg of heparin sulfate at 37°C for 1 h. Subsequently, 4 µl of 6× loading buffer (50% glycerol, 1% bromophenol blue, and 1% xylene cyanol FF in Tris/Borate/EDTA buffer) was added, and the samples were loaded onto 2% agarose gels containing 0.05 mg/ml ethidium bromide. Electrophoresis was performed at 130 mV and approximately 52 mA for 15 min, and the resulting gels were photographed under UV-illumination. The pictures were digitized and analyzed with Scion image analysis software (Meyer Instruments, Inc., TX, USA) to determine the mean density of the siRNA bands.

The dissociation curve was generated by plotting the percentage of siRNA dissociated from the complex versus heparin: polymer ratio (μg/μg). Results were presented as average of at least two independent experiments.

Assessing the cellular association of polymer/siRNA micelles by flow cytometry

To assess the uptake of polymer/siRNA micellar complexes into MDA-MB-435 cells, 5-carboxyfluorescein (FAM)-labeled scrambled siRNA was complexed with PEO-*b*-P(CL-*g*-SP) and PEO-*b*-P(CL-*g*-SP-Chol) at polymer:siRNA ratios of 16:1 (w/w) by incubation in water (corresponding 100 nM siRNA and 22.4 μg/ml polymer in culture medium) or with PEI25K in 1:1 weight ratio as positive control, and their cellular association was measured by flow cytometry according to a method described previously [17].

Assessing the cellular uptake & distribution of siRNA by confocal microscopy

Confocal microscopy was used to assess the intracellular trafficking of siRNA in MDA-MB-435 cells. Micelles were prepared using FAM-labeled scrambled siRNA complexed with PEO-*b*-P(CL-*g*-SP) and PEO-*b*-P(CL-*g*-SP-Chol) at polymer:siRNA ratios of 16:1 (w/w) by incubation in water (corresponding 100 nM siRNA and 22.4 μg/ml polymer in culture medium), and their association in MDA-MB-435 cells was assessed using confocal microscopy according to a previously described method [17].

Cytotoxicity evaluation by MTT assay

The cytotoxicity of various polymeric micelles against MDA-MB-435 cells was monitored using MTT assay [42]. Scrambled siRNA was used to make polymer/siRNA micelles at ratios of 8:1, 16:1 and 32:1 (w/w) polymer to siRNA. MDA-MB-435 cells were seeded in 24-well plates with 0.4 ml medium in each well, and allowed to reach approximately 80% confluence (24 h). The cells were then incubated for 24 h with polymer/siRNA micelles to give final polymer concentrations of 11.2, 22.4 and 44.8 μg/ml in triplicate. Untreated cells were used as control. After incubation for 24 h, 60 μl of MTT solution (5 mg/ml in HBSS) was added to each well and reincubated for 2 h at 37°C. The residual MTT solution was removed, and 300 μl of DMSO was added to each well to dissolve the formed crystals. The percentage cell viability was determined by measuring the optical density of the wells at 570 nm using a Power Wave X 340 microplate reader (BioTek Instruments, VT, USA) with cell-less medium as a blank, and comparing these values to the untreated cells.

Assessing the silencing activity of MCL-1 siRNA micelles by real-time PCR

Real-time (RT) PCR was carried out to determine *MCL-1* knockdown at the mRNA level in MDA-MB-435 cells at 48 h, using scrambled and MCL-1 siRNA at polymer:siRNA ratio of 16:1 (w/w) (final polymer and siRNA concentration of 11.2 μg/ml and 50 nM per well) according to a procedure described earlier [17].

In vitro therapeutic efficacy of MCL-1 siRNA micelles

The cytotoxicity of MCL-1 and scrambled siRNA complexed with different polymers as a measure of therapeutic efficacy was evaluated in MDA-MB-435 cells using MTT assay as described above. siRNA micelles were prepared using the scrambled and MCL-1 siRNA at polymer:siRNA ratios of 16:1 (w/w) and were added to the wells (final polymer concentration of 11.2 μg/ml and siRNA concentrations of 50 nM per well in triplicate wells). Cells were incubated for 72 h in their normal maintenance conditions and then 60 μl of MTT solution (5 mg/ml in HBSS) was added to each well. After 2 h of incubation in 37°C, the medium was removed, and 300 μl of DMSO was added to each well to dissolve the crystals formed. The optical density of the wells was measured at 570 nm using a Power Wave X 340 microplate reader with cell-less medium as blank, and comparing these values to the untreated cells.

Animal models

Female athymic NCr nude mice were purchased from Taconic Biosciences, Inc. (NY, USA). All experiments were performed using 4- to 6-week-old female mice. All animal studies were conducted in accordance with the guidelines of the Canadian Council on Animal Care with approval from the Animal Care and Use Committee of the University of Alberta (AB, Canada). To establish the tumor model, mice were randomly assigned into five groups of six mice per group. Mice were inoculated with 2×10^6 MDA-MB-435 cells in a volume of 50 μl PBS injected subcutaneously in the right rear flank. The mice were used when the tumors reached a size of 100 mm^3 (10 days after injection).

In vivo activity of MCL-1 siRNA micelles after intratumoral & intravenous injection

Tumor-bearing mice were either treated intratumorally or intravenously with siRNA polymeric micellar formulations. For intratumoral injections, mice-bearing tumors were injected with 50 μl HEPES, 10 μg scrambled or MCL-1 siRNA-loaded micelles. For intravenous injections, mice-bearing tumors were injected via

tail vein with 100 µl dextrose, 40 µg MCL-1 siRNA loaded in plain or RGD4C-modified PEO-*b*-P(CL-*g*-SP) or PEO-*b*-P(CL-*g*-SP-Chol) micelles (refer to Table 3 for preparation of micellar complexes). For both experiments, treatment was given every third day for three doses (days 4, 7 and 10). Mice were monitored daily according to previously reported method [43]. Tumor size was measured on days 0, 4, 7, 10 and 13 with a caliper, and mean ± standard error of the mean of relative tumor volume in each group was calculated using the formula: tumor volume = $0.4LW^2$ (L is the long diameter and W is the short diameter of the tumor); and plotted as a function of time according to previously reported method [43]. Tumors were excised on day 13 and stored in RNAlater® solution (Life Technologies, Burlington, Ontario, Canada) at -20°C until further analysis.

RT-PCR was carried out on the excised tumors from both experiments to determine MCL-1 knockdown at the mRNA level. Tumors were homogenized and total RNA was extracted using RNeasy spin columns (Qiagen) according to the manufacturer's recommendations. cDNA was synthesized and RT-PCR was performed on a StepOnePlus™ RT-PCR system (Applied Biosystems, CA, USA) with β-actin as the endogenous housekeeping gene and the specific MCL-1 primers according to the procedure described above. Each sample was measured in triplicate.

To study the safety of the micellar complexes after intravenous administration, mice were monitored for their weights, and tissues (liver, spleen and kidneys) were excised for histological examination on day 13 and stored in 10% neutral buffered formalin until further use. For histological examination, the stored tissues were embedded in paraffin. Slices of 2-µm thickness were cut, deparaffinized, hydrated and stained with hematoxylin–eosin. Each slide was assigned a code number before being sent for microscopic assessment. The microscopic assessments were performed by a qualified veterinary pathologist, Dr PN Nation, DVM, PhD, DACVP from the Animal Pathology Services Ltd. The assessor, who was blinded to the treatment groups and to the nature of the study design, was asked to look for qualitative evidence of microscopic changes consistent with tissue toxicity. Tissues of three mice from each group were randomly chosen for histological examination.

Statistics

Values are presented as mean ± standard deviation or mean ± standard error of the mean. Statistical significance was tested using unpaired Student's *t*-test, or one-way analysis of variance (ANOVA) followed by Tukey's *post hoc* test as noted in the text. The level of significance was set at $\alpha \leq 0.05$.

Results

Synthesis & characterization of PEO-*b*-P(CL-*g*-SP-Chol)

The synthetic method for the preparation of PEO-*b*-P(CL-*g*-SP-Chol) is shown in Figure 1. Peaks corresponding to cholesteryl group of PEO-*b*-P(CL-*g*-SP-Chol) polymer were observed at δ = 0.84–1.1 and 5.35 ppm in the ^{1}H NMR spectra, indicating the successful conjugation of cholesteryl groups to the block copolymer (Figure 2B). Based on peak intensity ratio of proton from PCL (-OCH_2- proton, δ = 4.1 ppm) to the intensity of specific peak in PEO (-CH_2CH_2O- proton, δ = 3.65 ppm), degree of polymerization of PCL block was calculated to be 15. For PEO-*b*-P(CL-*g*-SP) copolymer, the number of SPs on the PCL block was determined to be 6. In other words, approximately 40% of carboxyl groups were substituted with SP. On average, the substitution level of cholesteryl group on the SP was also around 40% (i.e., 2.4 out of 6 SPs). This polymer is shown as PEO_{114}-*b*-P(CL-*g*-SP-Chol)$_{15–6–2.4}$ where 15–6–2.4 refers to the degree of caprolactone polymerization, the number of conjugated SP groups and the number of cholesteryl substituted SPs in the subscript, respectively.

As expected, owing to the hydrophobicity of cholesteryl substituent, the CMC of PEO-*b*-P(CL-*g*-SP-Chol) (0.092 µM) was significantly lower than that of PEO-*b*-P(CL-*g*-SP) (0.67 µM) (unpaired Student's

Table 1. Characteristics of prepared block copolymers (n = 3).

Polymer	Cholesteryl substitution on SP%†	M_n‡g/mol	CMC§±SD (µM)
PEO_{114}-*b*-P(CL-*g*-SP-Chol)$_{15–6–2.4}$	40	9400	0.09 ± 0.01¶
PEO_{114}-*b*-P(CL-*g*-SP)$_{15–6}$	NA	8552	0.67 ± 0.05

†Mole percent.
‡Determined by ^{1}H NMR.
§Measured from the onset of a rise in the intensity ratio of peaks at 339 nm to peaks at 334 nm in the fluorescence excitation spectra of pyrene plotted versus logarithm of polymer concentration.
¶Indicates statistical significance between PEO-*b*-P(CL-*g*-SP-Chol) and PEO-*b*-P(CL-*g*-SP) (unpaired Student's *t*-test, $p < 0.05$)
CMC: Critical micellar concentration; NA: Not applicable; PEO-*b*-P(CL-*g*-SP): Poly(ethylene oxide)-*block*-poly(ε-caprolactone-*grafted*-spermine); PEO-*b*-P(CL-*g*-SP-Chol): Poly(ethylene oxide)-*b*-poly(ε-caprolactone-*g*-N-(spermine)-cholesteryl carboxylate); SD: Standard deviation; SP: Spermine.

Table 2. Characteristics of prepared block copolymer micelles (n = 3).

Polymeric micelles	Size† ± SD (nM)	ζ-potential‡ ± SD (mV)
PEO-*b*-P(CL-*g*-SP-Chol)	28 ± 5.0	2.50 ± 0.09§
PEO-*b*-P(CL-*g*-SP)	40 ± 10.0	1.70 ± 0.24
Acetal-PEO-*b*-P(CL-*g*-DP)/PEO-*b*-P(CL-*g*-SP-Chol)	65 ± 0.3	-0.06 ± 0.38
Acetal-PEO-*b*-P(CL-*g*-DP)/PEO-*b*-P(CL-*g*-SP)	69 ± 1.3	-0.37 ± 0.29
RGD-PEO-*b*-P(CL-*g*-DP)/PEO-*b*-P(CL-*g*-SP-Chol)	65 ± 0.6	-2.45 ± 0.88
RGD-PEO-*b*-P(CL-*g*-DP)/PEO-*b*-P(CL-*g*-SP)	70 ± 0.4	-1.60 ± 1.63

†Z-average estimated by DLS technique.
‡ζ-potential estimated by DLS technique.
§Indicates statistical significance between their unmodified counterpart (e.g., PEO-*b*-P(CL-*g*-SP-Chol) and PEO-*b*-P(CL-*g*-SP)) (unpaired Student's *t*-test, $p < 0.05$).
DLS: Dynamic light scattering; PEO-*b*-P(CL-*g*-SP): Poly(ethylene oxide)-*block*-poly(ε-caprolactone-*grafted*-spermine); PEO-*b*-P(CL-*g*-SP-Chol): Poly(ethylene oxide)-*b*-poly(ε-caprolactone-*g*-N-(spermine)-cholesteryl carboxylate); RGD: Arginylglycylaspartic acid; SD: Standard deviation.

t-test, $p < 0.05$) (Table 1). The Z-average diameter of PEO-*b*-P(CL-*g*-SP) micelles determined by the dynamic light scattering technique was 40 ± 10 nm (Table 2). On the other hand, micelles formed from PEO-*b*-P(CL-*g*-SP-Chol) exhibited smaller size, showing average diameter of 28 ± 5 nm (Table 2). This was despite presence of bulky cholesteryl groups on the core-forming block of micelles. Similar change in size was seen in the TEM images (Supplementary Figure 1). The images showed the formation of true spherical structures having a clear boundary. The average ζ-potential of PEO-*b*-P(CL-*g*-SP) micelles was 1.70 mV. On the other hand, PEO-*b*-P(CL-*g*-SP-Chol) micelles exhibited a significantly higher ζ-potential of 2.50 mV (unpaired Student's *t*-test, $p < 0.05$), despite partial conversion of primary amine groups in SP to secondary amines in SP-Chol.

RGD4C modification of the shell

Formation of mixed micelles from acetal-PEO-*b*-P(CL-*g*-DP)/PEO-*b*-P(CL-*g*-SP) and acetal-PEO-*b*-P(CL-*g*-DP)/PEO-*b*-P(CL-*g*-SP-Chol) led to a significant increase in micellar size when compared with micelles formed from single PEO-*b*-P(CL-*g*-SP) or PEO-*b*-P(CL-*g*-SP-Chol) micelles (Table 2). RGD4C modification, however, did not change the particle size of the micelles. The average ζ-potential of the micelles post addition of acetal-PEO-*b*-P(CL-*g*-DP) or RGD4C-PEO-*b*-P(CL-*g*-DP) was slightly negative when compared with that obtained by PEO-*b*-P(CL-*g*-SP) and PEO-*b*-P(CL-*g*-SP-Chol) (Table 2).

siRNA binding

As expected, the synthesized PEO-*b*-P(CL-*g*-SP) and PEO-*b*-P(CL-*g*-SP-Chol) copolymer were capable of effectively binding siRNA (Figure 3). When the polymer:siRNA ratios (w/w) were higher than 16:1, all the copolymers were capable of 100% siRNA binding. The binding ability of the synthesized copolymers were not significantly different from each other, but less than that of PEI25K as indicated by a significant left shift in binding versus polymer:siRNA weight ratio plot.

Table 3. Polymer compositions for the preparation of siRNA micellar complexes for *in vivo* studies.

Micelle compositions used for intratumoral injection		Micelle compositions used for intravenous injection	
Polymer composition	Composition ratio (W:W)†	Polymer composition	Composition ratio (W:W)†
SCR-SP micelles	I:V (16:1)	Plain-SP micelles	I:III:VI (16:32:1)
MCL-SP micelles	I:VI (16:1)	Plain-SP-Chol micelles	II:III:VI (16:32:1)
SCR-SP-Chol micelles	II:V (16:1)	RGD-SP micelles	I:IV:VI (16:32:1)
MCL-SP-Chol micelles	II:VI (16:1)	RGD-SP-Chol micelles	II:IV:VI (16:32:1)

†(I) PEO-*b*-P(CL-*g*-SP), (II) PEO-*b*-P(CL-*g*-SP-Chol), (III) acetal-PEO-*b*-P(CL-*g*-DP), (IV) RGD4C-PEO-*b*-P(CL-*g*-DP), (V) Scrambled siRNA, (VI) MCL-1 siRNA.
Chol: Cholesteryl carboxylate; MCL: Myeloid cell leukemia; PEO-*b*-P(CL-*g*-SP): Poly(ethylene oxide)-*block*-poly(ε-caprolactone-*grafted*-spermine); PEO-*b*-P(CL-*g*-SP-Chol): Poly(ethylene oxide)-*b*-poly(ε-caprolactone-*g*-N-(spermine)-cholesteryl carboxylate); SCR: Scrambled; SP: Spermine; w:w: Weight/weight.

Release of siRNA from polymer/siRNA micelles upon challenge with heparin

As shown in Figure 4, the siRNA release was dependent on heparin concentration. The heparin:polymer ratio (μg/μg) which led to 50% siRNA release (RR_{50}) from the complexes was used as a measure of propensity for dissociation. PEO-*b*-P(CL-*g*-SP) exhibited slightly slower release of siRNA compared with PEO-*b*-P(CL-*g*-SP-Chol), based on the higher RR_{50} values for the former polymer (0.2 μg/μg heparin:polymer) as compared with the RR_{50} value of 0.1 μg/μg for PEO-*b*-P(CL-*g*-SP-Chol). All polymer/siRNA complexes exhibited higher siRNA release compared with PEI25K/siRNA complex (RR_{50} = 4.12 μg/μg, heparin:polymer), even though the latter was prepared at a low 1:1 polymer:siRNA ratio (w/w).

Cellular association & uptake studies

In general, complexation of siRNA with all polymers under study was found to be effective in increasing the association of siRNA with cells as the percentage of siRNA-positive cells reached its maximum level within 24 h following complexation with either PEI25K or polymeric micelles (Figure 5A & B). Based on the mean fluorescent intensity data, PEI25K was significantly more effective (one-way ANOVA followed by Tukey's *post hoc* test, $p < 0.05$) than PEO-*b*-P(CL-*g*-SP) and PEO-*b*-P(CL-*g*-SP-Chol) in delivering siRNA to MDA-MB-435 cells at both 3 and 24 h (Figure 5). Substitution of cholesteryl on PEO-*b*-P(CL-*g*-SP) also resulted in significantly higher siRNA delivery to MDA-MB-435 cells (maximum mean fluorescence intensity) at 3 h and 24 h compared with its PEO-*b*-P(CL-*g*-SP) counterpart (one-way ANOVA; Tukey's *post hoc* test; $p < 0.05$) (Figure 5C & D).

Confocal microscopy was then used to investigate the cellular distribution of polymer/siRNA micelles in MDA-MB-435 cells (Figure 6). Clear green-colored siRNA fluorescence was observed in cytoplasm when siRNA was formulated in PEO-*b*-P(CL-*g*-SP-Chol) micelles (Figure 6A), while siRNA alone (Figure 6A) exhibited no detectable fluorescence in the cells. The observation of yellow color in the merged fluorescence images (Figure 6D) due to the FAM-labeled siRNA (green, Figure 6A) and LysoTracker (red, Figure 6C) for PEO-*b*-P(CL-*g*-SP-Chol)/siRNA complexes implies internalization of these micelles into cells by endocytosis and partial localization of siRNA in the endosomes.

Cytotoxicity of synthesized polymers

Overall, cholesteryl substitution on PEO-*b*-P(CL-*g*-SP) significantly decreased the nonspecific cytotoxicity of these polymers (Figure 7). All polymeric micellar siRNA complexes under study exhibited minimal cytotoxicity (<20%) at polymer:siRNA ratio of 8:1 (w/w) with 100 nM of siRNA. At polymer:siRNA 16:1 ratio (w/w) and 100 nM siRNA, PEO-*b*-P(CL-*g*-SP) micelles caused approximately 40% cytotoxicity, while PEO-*b*-P(CL-*g*-SP-Chol) caused only approximately 20% cytotoxicity (unpaired Student's *t* -test, $p < 0.05$).355393

MCL-1 knockdown by polymeric micellar siRNAs

MDA-MB-435 were treated for 48 h with 50 nM siRNA at a polymer:siRNA ratio of 16:1 (w/w). At 48 h, the level of MCL-1 mRNA expression after incubation with MCL-1 siRNA/PEO-*b*-P(CL-*g*-SP-Chol) micelles was reduced by approximately 98% compared with untreated control group (Figure 8). This was significantly different from identical scrambled-siRNA/PEO-*b*-P(CL-*g*-SP-Chol) micelles, which decreased MCL-1 mRNA expression by 55% (unpaired Student's *t*-test, $p < 0.05$). MCL-1 siRNA/PEO-*b*-P(CL-*g*-SP) micelles reduced MCL-1 mRNA expression by approximately 90%. The level of MCL-1 mRNA knockdown was significantly different from identical scrambled-siRNA/PEO-*b*-P(CL-*g*-SP) micelles, which decreased MCL-1 mRNA expression by 42% (unpaired Student's *t*-test, $p < 0.05$). The level of MCL-1 mRNA expression after incubation with MCL-1 siRNA/PEO-*b*-P(CL-*g*-SP-Chol) micelles was lower than that for MCL-1 siRNA/PEO-*b*-P(CL-*g*-SP) micelles (unpaired Student's *t*-test, $p < 0.05$), signifying better *MCL-1* silencing by PEO-*b*-P(CL-*g*-SP-Chol), *in vitro*.

The effect of *MCL-1* silencing by MCL-1 siRNA polymeric micelles on the viability of MDA-MB-435 cells

MCL-1 siRNA/PEO-*b*-P(CL-*g*-SP-Chol) micelles with 50 nM siRNA and polymer:siRNA ratio of 16:1 (w/w) caused 47% MCL-1-associated inhibition of cell growth (Figure 9). This level of inhibition was significantly different from scrambled siRNA/PEO-*b*-P(CL-*g*-SP-Chol) micelles, which caused 20% nonspecific inhibition of cell growth (unpaired Student's *t*-test, $p < 0.05$). MCL-1 siRNA/PEO-*b*-P(CL-*g*-SP) polymeric micelles with the same siRNA dose and polymer:siRNA ratio did not exhibit any MCL-1-associated inhibition of cell growth. Inhibition of cell growth caused by MCL-1 siRNA/PEO-*b*-P(CL-*g*-SP-Chol) was significantly higher from that caused by MCL-1 siRNA/PEO-*b*-P(CL-*g*-SP) complexes.

Figure 2. 1H NMR spectra of polymers under study for siRNA delivery. ^{1}H NMR spectra of **(A)** PEO-*b*-P(CL-*g*-SP) in D_2O and **(B)** PEO-*b*-P(CL-*g*-SP-Chol) in $CDCl_3$ and peak assignments. PEO-*b*-P(CL-*g*-SP): Poly(ethylene oxide)-*block*-poly(ε-caprolactone-*grafted*-spermine); PEO-*b*-P(CL-*g*-SP-Chol): Poly(ethylene oxide)-*b*-poly(ε-caprolactone-*g*-N-(spermine)-cholesteryl carboxylate).

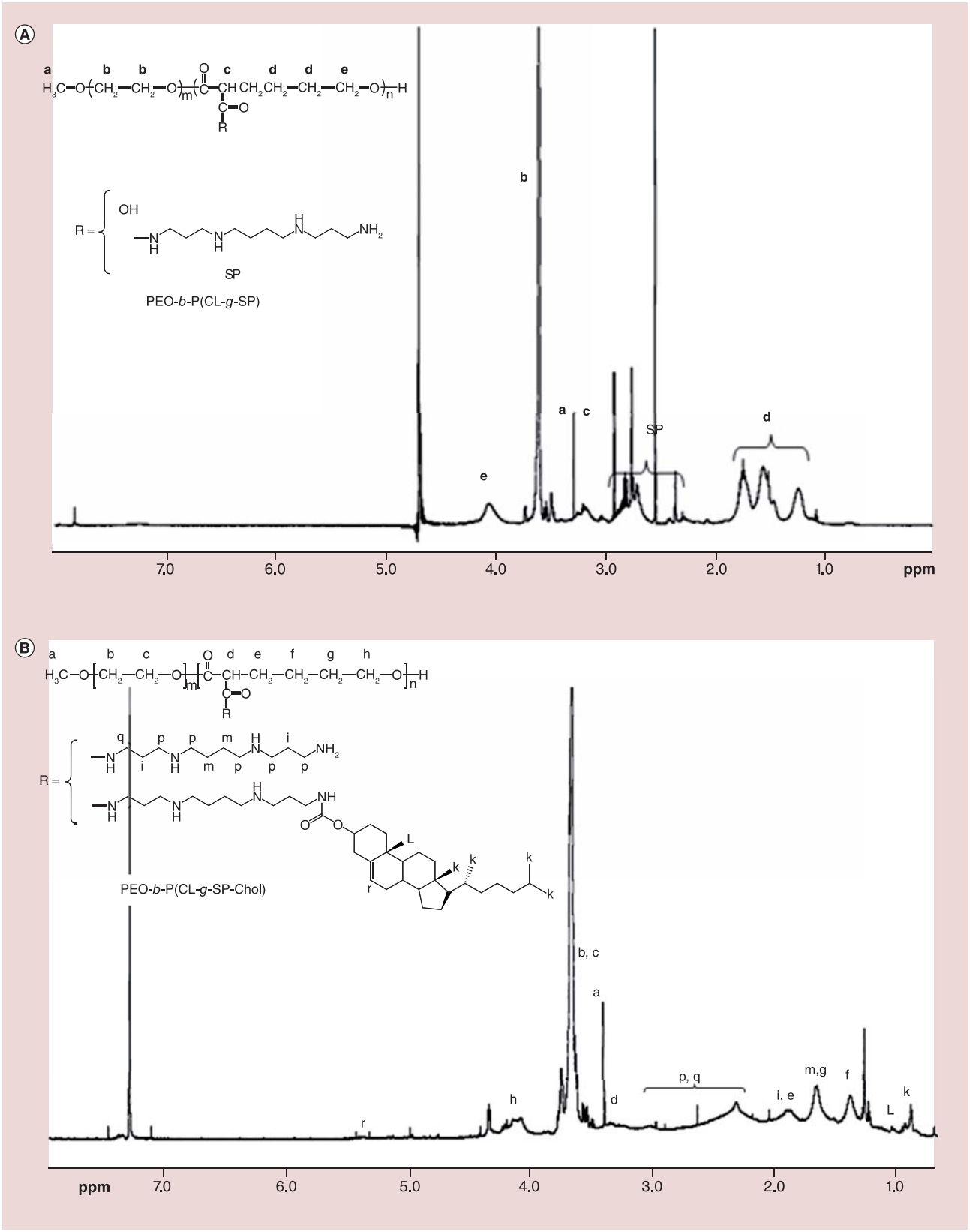
A
a b b c d d e
OH
R =
SP
PEO-b-P(CL-g-SP)
b
a c
SP
d
e
7.0 6.0 5.0 4.0 3.0 2.0 1.0 ppm
B
a b c d e f g h
q p p m i
R =
PEO-b-P(CL-g-SP-Chol)
L
k
r
b, c
a
h
d
p, q
i, e
m,g
f
k
L
ppm 7.0 6.0 5.0 4.0 3.0 2.0 1.0

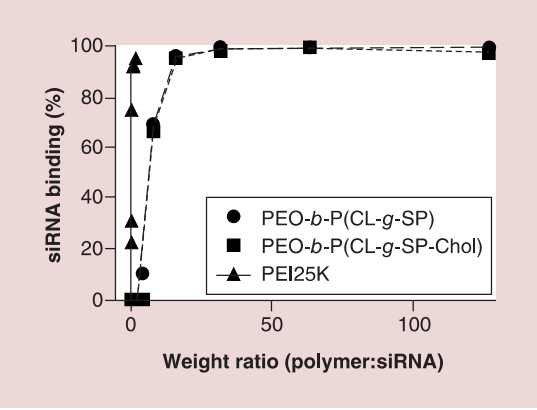

Figure 3. The binding affinity of different polymers to scrambled siRNA. Percentage of siRNA binding versus polymer:siRNA weight ratios is shown (n = 3).

In vivo activity of MCL-1 siRNA micelles following intratumoral injection

The composition of test-treatment groups in this study is summarized in Table 3. As shown in Figure 10A, the level of MCL-1 mRNA expression after treatment with MCL-SP-Chol micelles was reduced by approximately 38% compared with untreated control group and SCR-SP-Chol micelles, which showed no decrease in MCL-1 mRNA expression (one-way ANOVA followed by Tukey's *post hoc* test, $p < 0.05$). MCL-SP micelles were effective in reducing MCL-1 mRNA expression by approximately 31% compared with untreated control group and SCR-SP micelles which showed no decrease in MCL-1 mRNA expression (one-way ANOVA followed by Tukey's *post hoc* test, $p < 0.05$). The difference in downregulation of MCL-1 mRNA by MCL-SP-Chol micelles was not statistically significant from that of MCL-SP micelles (one-way ANOVA followed by Tukey's *post hoc* test, $p > 0.05$).

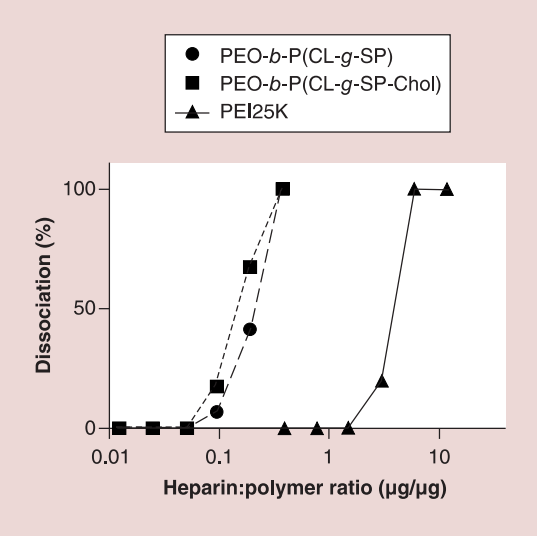

Figure 4. siRNA release from different micelles by heparin competition. Scrambled siRNA was complexed with various polymers at 32:1 polymer:siRNA ratio (w/w) and with PEI25K at 1:1 ratio (w/w). Amount of complex dissociation was determined with assessing free siRNA by agarose gel electrophoresis (n = 3). w/w: Weight/weight.

To evaluate the effect of *MCL-1* silencing at mRNA level on tumor growth, tumor volumes were measured on days 0, 4, 7, 10 and 13. In general, both MCL-SP-Chol and MCL-SP micelles were able to retard the growth of the tumor upto day 10, following which the tumor started to grow again (Figure 10B). This might be due to the compensating effect of other antiapoptotic factors in the treated tumor at this point. On day 13, MCL-SP and MCL-SP-Chol micelles showed a 1.9- and 3.5-fold decrease in tumor volume, respectively. However, this decrease in tumor volume was statistically not different from that of the untreated group and the scrambled counterparts (one-way ANOVA followed by Tukey's *post hoc* test, $p > 0.05$). Although treatment with MCL-SP-Chol micelles resulted in a significant decrease in tumor volume compared with untreated group on day 10, this decrease in tumor volume was not significantly different from MCL-SP micelles (one-way ANOVA followed by Tukey's *post hoc* test; $p > 0.05$).

In vivo activity of RGD4C-functionalized versus plain MCL-1 siRNA micelles after intravenous injection

The composition of test treatment groups in this study is summarized in Table 3. The choice of RGD4C-modified micellar siRNA as test groups in this study was based on our previous result, which has shown high accumulation and targeting of RGD4C-modified PEO-*b*-P(CL-*g*-SP) micelles in the same tumor model following intravenous administration [15]. RGD4C was successfully conjugated to the micellar shell of PEO-*b*-P(CL-*g*-SP) and PEO-*b*-P(CL-*g*-SP-Chol) micelles at a conjugation efficiency of 100% w/w. The conjugation density, that is, molar ratio of peptide to the polymer, was approximately 20%.

The RGD4C modification of polymeric micellar siRNA complexes was shown to enhance the silencing activity of complexed siRNA in MDA-MB-435 xenografts following intravenous injection. Cholesterol modification of the core, however, did not affect the silencing activity of complexed siRNA under the same conditions. As shown in Figure 11A, the level of MCL-1 mRNA expression after treatment with RGD-SP-Chol micelles was reduced by approximately 36% compared with untreated control group (one-way ANOVA followed by Tukey's *post hoc* test, $p < 0.05$). This level of *MCL-1* knockdown was significantly dif-

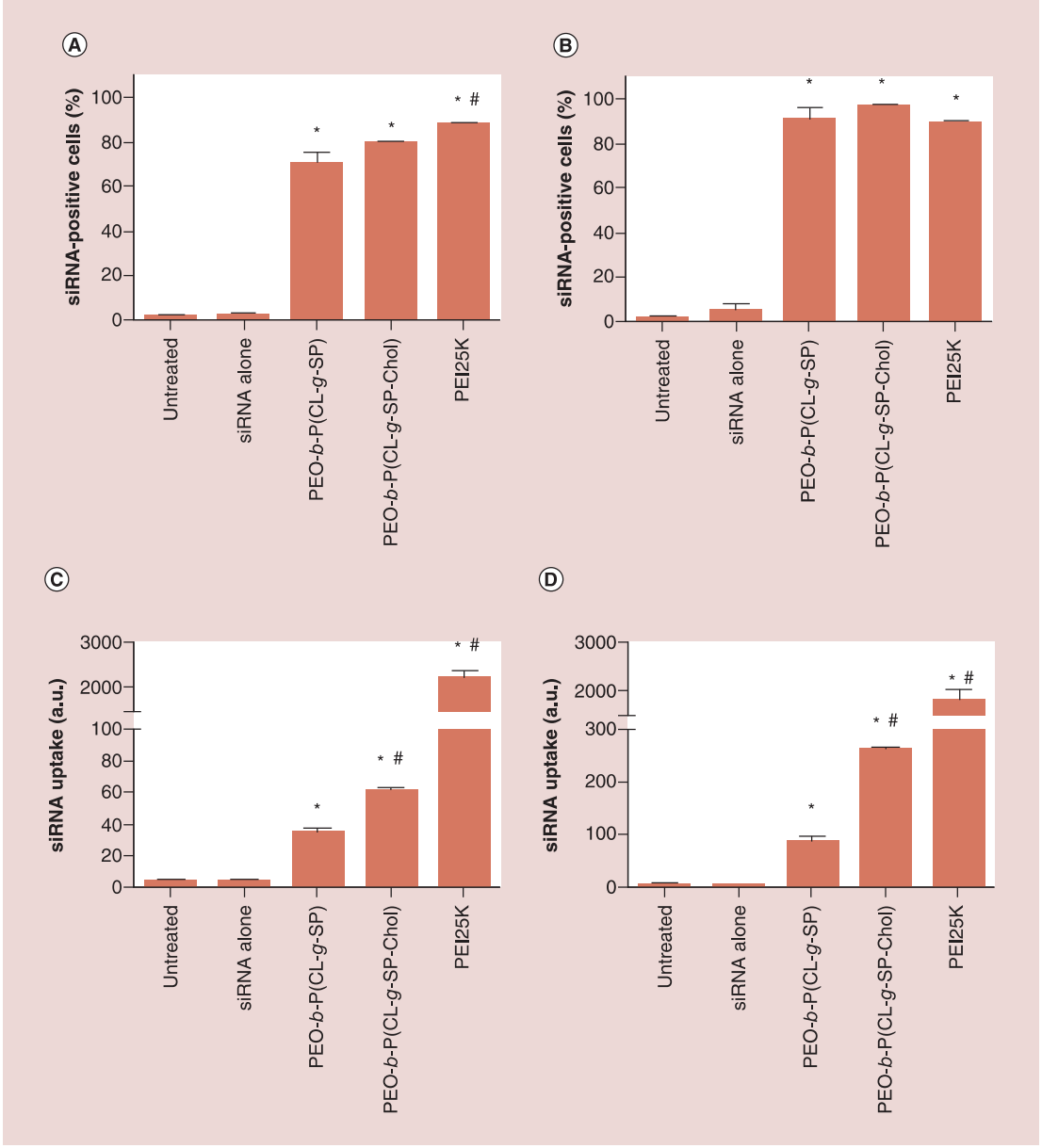

Figure 5. Cellular uptake of polymer/carboxyfluorescein–siRNA complexes by MDA-MB-435 cells. The percentage of cells positive for FAM-siRNA after **(A)** 3 h and **(B)** 24 h exposure to siRNA micelles, and the mean fluorescence intensity of the cells after **(C)** 3 h and **(D)** 24 h exposure to siRNA micelles at PEO-*b*-P(CL-*g*-SP):siRNA or PEO-*b*-P(CL-*g*-SP-Chol):siRNA ratios of 16:1 (w/w) and PEI25K:siRNA ratio of 1:1 (w/w). The data are the mean ± standard error of the mean for *n = 3*.*Significantly different from siRNA alone ($p < 0.05$).
#Significantly different from PEO-*b*-P(CL-*g*-SP) ($p < 0.05$). One-way ANOVA followed by Tukey's *post hoc* test, $p < 0.05$.
FAM: Carboxyfluorescein; PEO-*b*-P(CL-*g*-SP): Poly(ethylene oxide)-*block*-poly(ε-caprolactone-*grafted*-spermine); PEO-*b*-P(CL-*g*-SP-Chol): Poly(ethylene oxide)-*b*-poly(ε-caprolactone-*g*-N-(spermine)-cholesteryl carboxylate); w/w: Weight/weight.

ferent from plain-SP-Chol micelles, which showed only approximately 12% decrease in MCL-1 mRNA expression (one-way ANOVA followed by Tukey's *post hoc* test, $p < 0.05$). RGD-SP micelles were effective in reducing MCL-1 mRNA expression by approximately 40% compared with untreated control group (one-way ANOVA followed by Tukey's *post hoc* test, $p < 0.05$). This level of *MCL-1* knockdown was sig-

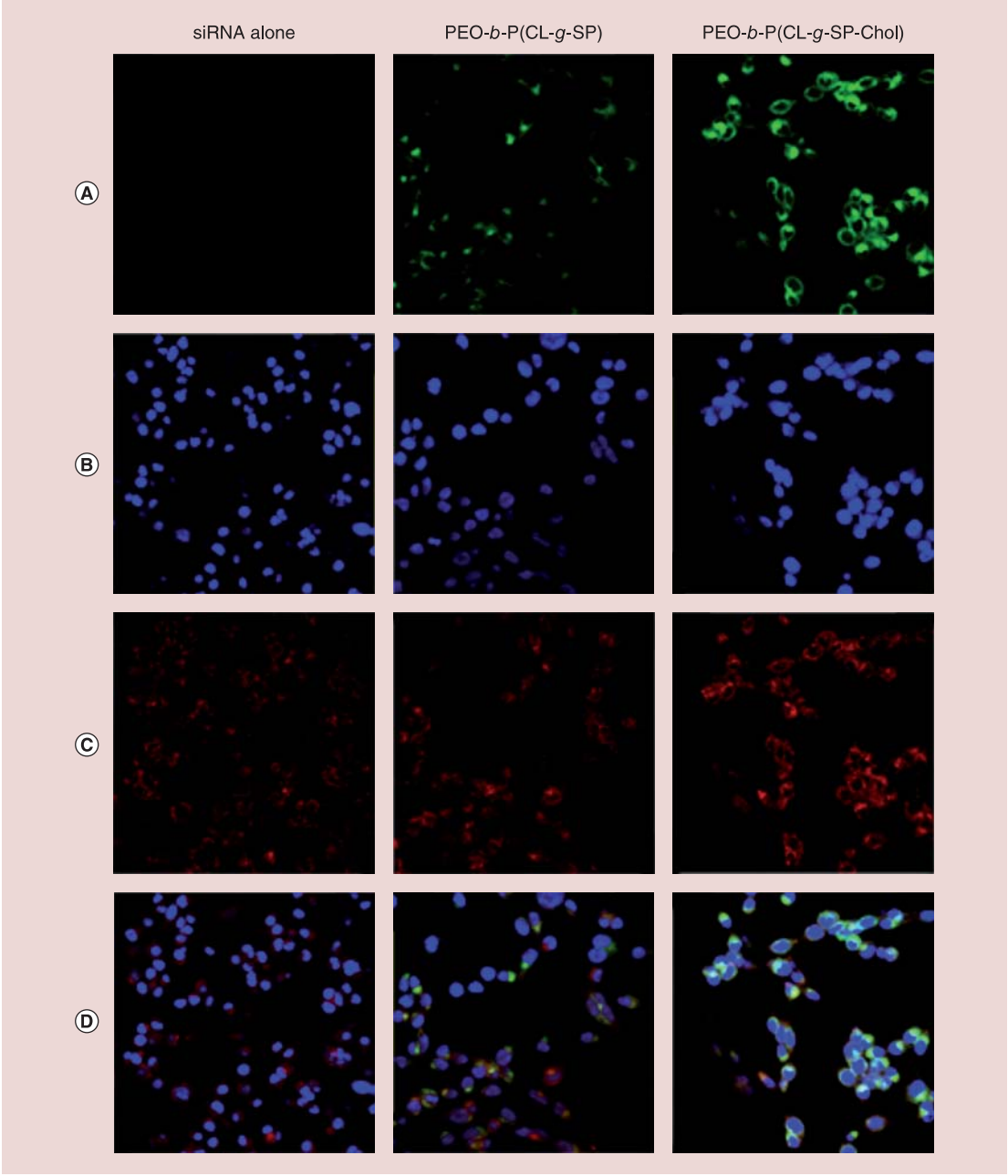

Figure 6. Cellular distribution of polymer/siRNA micelles by confocal microscopy. Uptake and intracellular distribution of FAM-siRNA formulated in micelles by MDA-MB-435 cells using confocal microscopy. The observation was done after 24 h exposure to FAM-siRNA alone or formulated with PEO-*b*-P(CL-*g*-SP) or PEO-*b*-P(CL-*g*-SP-Chol) at polymer:siRNA ratios of 16:1 (w/w). **(A)** Images represent FAM-siRNA (green) alone. **(B)** Images represent nucleus stained with DAPI (blue). **(C)** Images represent lysosomes stained with lysoTracker (red) and **(D)** represents images merged together.
DAPI: 4′,6-diamidino-2-phenylindole; FAM: Carboxyfluorescein; PEO-*b*-P(CL-*g*-SP): Poly(ethylene oxide)-*block*-poly(α-carboxylate-ε-caprolactone-*grafted*-spermine); PEO-*b*-P(CL-*g*-SP-Chol): Poly(ethylene oxide)-*b*-poly(ε-caprolactone-*g*-N-(spermine)-cholesteryl carboxylate); w/w: Weight/weight.

nificantly different from identical plain-SP micelles, which showed approximately 20% decrease in MCL-1 mRNA expression (one-way ANOVA followed by Tukey's *post hoc* test, $p < 0.05$). Both RGD-SP-Chol and plain-SP-Chol micelles showed similar *MCL-1* knockdown when compared with RGD-SP and plain-

SP counterparts, respectively, (one-way ANOVA followed by Tukey's *post hoc* test, $p > 0.05$) indicating that cholesterol modification of PEO-*b*-P(CL-*g*-SP) had no effect on the *MCL-1* knockdown after systemic delivery. This was similar to results seen after intratumoral injection, but different from what we observed *in vitro*. Mice treated with polymer/MCL-1 siRNA complexes with or without RGD4C functionalization at the surface showed retardation trend in tumor growth rate, however, the relative tumor volumes of the treated test groups were not significantly different from the control group (one-way ANOVA followed by Tukey's *post hoc* test, $p > 0.05$) (Figure 11B).

The weight of the animals increased during the study indicating that the mice tolerated the regimen well (Figure 11C). The organs of most mice in the treatment groups were microscopically normal (Figure 11D). One mouse each from plain-SP and RGD-SP micelles group had minimal hyperplasia of the lymphoid germinal centers. This, however, is a normal physiological reaction of the spleen, and as there was no particular group-associated pattern, it was concluded not to be related to the formulations. All formulations were found to have no adverse toxic effects on the mice during the duration of this study.

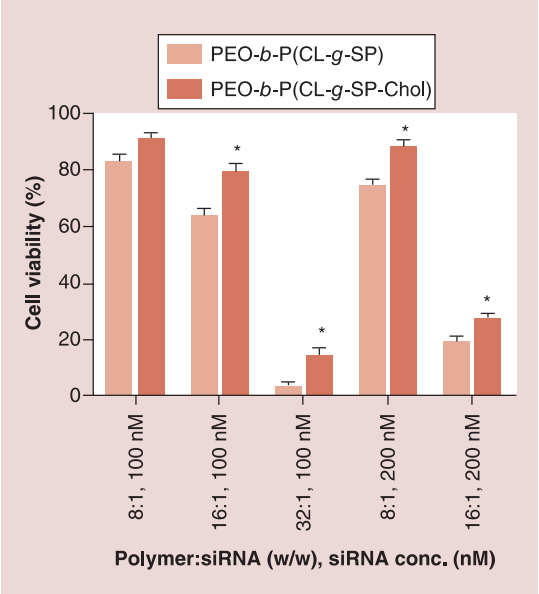

Figure 7. Cytotoxicity of the synthesized block copolymers/scrambled siRNA complexes against MDA-MB-435 cells. Incubation time was 72 h. 8:1, 16:1 and 32:1 ratios represent polymer:siRNA ratio (w/w). 100 and 200 nM indicate the dose of siRNA used in each well. The data are the mean ± standard error of the mean for n = 3.
*Significantly different from PEO-*b*-P(CL-*g*-SP) (unpaired Student's *t*-test, $p < 0.05$).
PEO-*b*-P(CL-*g*-SP): Poly(ethylene oxide)-*block*-poly(α-carboxylate-ε-caprolactone-*grafted*-spermine); w/w: Weight/weight.

Discussion

Advancement of siRNA technology for use in preclinical cancer models and in a clinical setting has been challenging due to the difficulty in the safe and effective delivery of siRNA to cancer cells following systemic administration [44]. Our research group has previously reported on the preparation of a siRNA delivery system for use in cancer-targeted siRNA delivery following intravenous administration. This delivery system is based on PEO-*b*-PCL block copolymers-bearing polycations like SP [13,15] on the α-carbon of ε-caprolactone in the PCL block for siRNA complexation. Since the SP groups are attached to the PCL backbone, siRNA complexation with the SP group protects the siRNA by forming a block copolymer micelle in which the siRNA is encapsulated into the PCL core whereas PEO is in the outer shell. In previous studies, our research group also reported on the use of RGD4C peptide as ligand to modify the surface of PEO-*b*-P(CL-*g*-SP) micelles. This modification led to a reduction in the required dose of siRNA for gene silencing and also improved the accumulation of polymeric micelles in tumor [14,15]. In the current study, we pursued modification of SP groups on the PCL backbone with cholesterol moieties and investigated the effect of this approach on siRNA delivery and silencing activity by plain or RGD4C-modified micelles in *in vitro* and *in vivo* cancer models. Cholesterol modification of SP was hypothesized to lead to improvements in the stability, cell interaction and eventually gene silencing and therapeutic activity of developed polymeric micellar siRNA delivery system.

In general, our observations confirmed the validity of this hypothesis following *in vitro* cell treatments. The CMC and average diameter of micelles were reduced, and their positive ζ-potential was increased (albeit not to a very big extent, possibly due to abundant PEG chains on the micellar surface) following cholesteryl modification of the micellar core. All of these properties imply an improved assembly and/or stability for the cholesteryl-modified polymeric micellar siRNA delivery system. A decrease in the CMC of PEO-*b*-P(CL-*g*-SP-Chol) compared with PEO-*b*-P(CL-*g*-SP), was a result of hydrophobization of the core-forming block with cholesterol groups. This change clearly indicates the improved thermodynamic stability of PEO-*b*-P(CL-*g*-SP-Chol) [45,46]. The increase in the ζ-potential after cholesterol modification, on the other hand, can be attributed to an increase in the aggregation number of PEO-*b*-P(CL-*g*-SP-Chol) compared with PEO-*b*-P(CL-*g*-SP) micelles thus increasing the

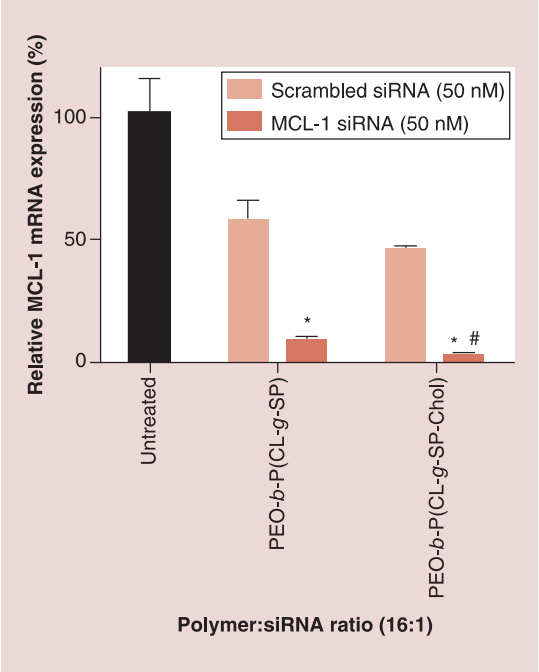

Figure 8. Myeloid cell leukemia-1 silencing activity of the myeloid cell leukemia-1 siRNA micelle complexes at mRNA level in MDA-MB-435 after 48 h by real-time PCR. The cells were transfected with MCL-1 or scrambled siRNA formulated in various micelles prepared using polymer:siRNA ratios of 16:1 (w/w) and 50 nM siRNA. Values are relative to untreated control. The data are the mean ± standard error of the mean (n = 3).
*Significantly different from its corresponding scrambled siRNA group (unpaired Student's *t*-test, $p < 0.05$).
#Significantly lower than MCL-1 siRNA/PEO-*b*-P(CL-*g*-SP) group (unpaired Student's *t*-test, $p < 0.05$).
MCL-1: Myeloid cell leukemia-1; PEO-*b*-P(CL-*g*-SP): Poly(ethylene oxide)-*block*-poly(α-carboxylate-ε-caprolactone-g-N-[spermine]); w/w: Weight/weight.

total positive charge on the micelle. Previous studies based on polystyrene-based micelles showed that an increase in the hydrophobicity of the insoluble polystyrene block was accompanied by a decrease in the CMC and an increase in the aggregation number of the micelles [47,48]. Further studies are needed to investigate this assumption. Nevertheless, the increase in the ζ-potential of cholesterol-substituted polymers is expected to lead to improved siRNA complexation by the modified polymeric micelle, and perhaps slower siRNA release. This might have contributed to our observation on the relatively similar binding of PEO-*b*-P(CL-*g*-SP) and PEO-*b*-P(CL-*g*-SP-Chol) to siRNA and similar siRNA release from both micellar structures despite partial conversion of primary amine groups in the latter polymer. The smaller size of PEO-*b*-P(CL-*g*-SP-Chol)/siRNA micelles may indicate formation of more compact micelles following siRNA complexation by cholesterol-modified polymer.

The increase in size of micelles after incorporation of acetal or RGD4C-modified PEO-*b*-P(CL-*g*-DP) might be due to the presence of bulky DP group [13]. The incorporation of the acetal-PEO-*b*-P(CL-*g*-DP) also led to a slightly negative ζ-potential due to the acetal group, which is similar to what has been reported in the literature [49,50].

Lipid modification is expected to enhance the interaction between the polymer/siRNA complexes and the hydrophobic domains of the plasma membrane facilitating cell uptake [16,17]. As expected, the cellular association of siRNA was higher when complexed with PEO-*b*-P(CL-*g*-SP-Chol) as compared with PEO-*b*-P(CL-*g*-SP). Confocal microscopy images confirmed the results of flow cytometry revealing better intracellular uptake of siRNA by PEO-*b*-P(CL-*g*-SP-Chol) micelles. Better uptake of cholesteryl-substituted polymeric micellar siRNA complexes may be attributed to the exposure of cholesteryl groups to the cell membrane leading to specific uptake by low-density lipoprotein receptors on cancer cells, and/or more compact structure of cholesteryl containing micellar siRNA complexes, altering uptake mechanism of the complexes. Cellular uptake of siRNA incorporated in PEO-*b*-P(CL-*g*-SP) or PEO-*b*-P(CL-*g*-SP-Chol), however, was much lower than PEI25K/siRNA complexes. This may be due to the hydrophilic PEG shell which shields the core positive charge thus reducing the interaction of polymeric micelles with cell membranes or other hydrophobic surfaces in a nonspecific manner [13,51].

Both, PEO-*b*-P(CL-*g*-SP) and PEO-*b*-P(CL-*g*-SP-Chol) also appeared to be successful in delivering siRNA into cytoplasm. According to previous literature, PEI25K has been found to deliver siRNA to both cytoplasm and nucleus [13,17]. Accumulation of siRNA in the cytoplasm where the target mRNA is located, rather than in the nucleus, provides an advantage for both, PEO-*b*-P(CL-*g*-SP) and PEO-*b*-P(CL-*g*-SP-Chol) over PEI25K in siRNA delivery.

Nonspecific cytotoxicity is a major concern for polycations employed for siRNA delivery. We studied the effect of cholesteryl substitution on the polycationic structure of PEO-*b*-P(CL-*g*-SP) micelles on nonspecific toxicity of developed micellar siRNA delivery systems by MTT assay. In general, complexes prepared at higher polymer:siRNA ratios (w/w) showed significantly higher cytotoxicity. This can be due to a higher net positive charge for the complexes at higher polymer:siRNA ratios [52]. Cholesteryl modification of PEO-*b*-P(CL-*g*-SP), however, decreased the cytotoxicity of polymeric micellar siRNA complexes, perhaps by

converting the primary amines in PEO-*b*-P(CL-*g*-SP) partially to secondary amines in PEO-*b*-P(CL-*g*-SP-Chol) and/or making more compact micelles.

Based on these results, a polymer:siRNA ratios of 16:1 (w/w) and MCL-1 siRNA doses of 50 nM were chosen to evaluate *MCL-1* silencing-associated specific cytotoxicity in further studies. Both, PEO-*b*-P(CL-*g*-SP) and PEO-*b*-P(CL-*g*-SP-Chol)/siRNA complexes yielded significantly better silencing of *MCL-1* in MDA-MB-435 cells when compared with polymer complexes with scrambled siRNA. Cholesteryl substitution, however, significantly enhanced the silencing activity of complexed MCL-1 siRNA at the mRNA level. This is in line with the increased cellular uptake of cholesteryl-substituted polymer/siRNA complexes by the same cell line compared with PEO-*b*-P(CL-*g*-SP) complexes of siRNA.

MCL-1 is key regulator of apoptosis and is shown to be essential for the survival of a variety of cell types. Silencing of *MCL-1* might be sufficient to promote apoptosis in cancer cells [28]. In our study, PEO-*b*-P(CL-*g*-SP-Chol)/siRNA complexes were able to both downregulate MCL-1 mRNA at 48 h incubation and also show significantly higher MCL-1-associated inhibition of cell growth compared with their scrambled siRNA complex counterparts following 72 h treatment. Under identical conditions, however, significant MCL-1-associated inhibition of cell growth following treatment of cells with PEO-*b*-P(CL-*g*-SP) micellar siRNA was not observed. This was despite significant downregulation of *MCL-1* mRNA expression by PEO-*b*-P(CL-*g*-SP)/siRNA complexes in MDA-MB-435 cells. The reason behind this observation is not clear, but may be attributed to the recovery of cells at longer time points following treatment with PEO-*b*-P(CL-*g*-SP)/MCL-1 siRNA micellar complexes or compensation of other antiapoptotic factors in treated cells for the effect of *MCL-1* silencing.

Intratumoral injection of MCL-1 siRNA complexed with PEO-*b*-P(CL-*g*-SP) and PEO-*b*-P(CL-*g*-SP-Chol) produced similar trends to *in vitro* results in terms of MCL-1 mRNA downregulation, with MCL-1 siRNA complexes of PEO-*b*-P(CL-*g*-SP-Chol) showing slightly better downregulation of MCL-1 mRNA expression over PEO-*b*-P(CL-*g*-SP) complexes, but the difference was not statistically significant. In line with the decreased expression of MCL-1 mRNA by polymeric micellar MCL-1 siRNA complexes, a decrease in the rate of tumor growth was also observed. However, again the slight better inhibition of tumor growth by the siRNA complexes with PEO-*b*-P(CL-*g*-SP-Chol) over PEO-*b*-P(CL-*g*-SP) complexes was statistically insignificant due to large variations in tumor growth among each group. The tumor growth inhibition by MCL-1 siRNA delivery was reduced after the 3rd injection of siRNA complexes by both polymeric micellar siRNA delivery systems, particularly that of PEO-*b*-P(CL-*g*-SP) formulations. Similar results were seen previously by Aliabadi *et.al.* using lipid-modified PEI/MCL-1 siRNA complexes [35]. This may reflect a compensating effect by other antiapoptotic factors for the silencing of *MCL-1*.

Following systemic intravenous administration, cholesterol modification of the core in PEO-*b*-P(CL-*g*-SP) did not impact the gene silencing or therapeutic activity of MCL-1 siRNA complexes in tumor xenografts. But the RGD4C modification of the micellar shell did improve the silencing activity of the polymeric micellar siRNA delivery systems for both PEO-*b*-P(CL-*g*-SP-Chol) and PEO-*b*-P(CL-*g*-SP) in tumor xenografts. This is perhaps due to increased accumulation of RGD4C-coated micelles in MDA-MB-435 tumors, in which $\alpha_V\beta_3$ integrin is overexpressed [53–55], as shown in our previous study [15]. The downregulation of MCL-1 mRNA expression in tumor xenografts following intravenous administration of MCL-1 siRNA complexes with RGD4C-modified micelles was not sufficient to cause significant inhibition of

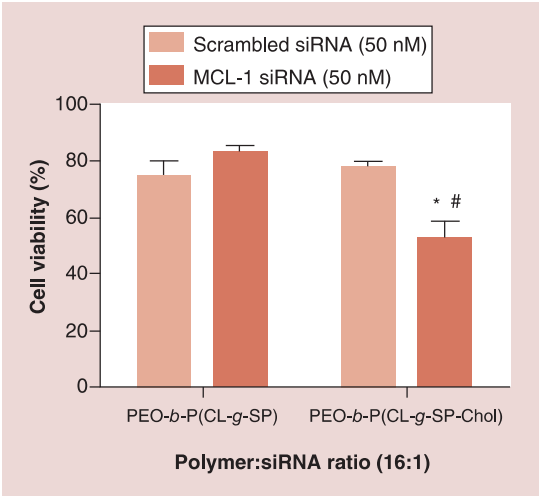

Figure 9. Cytotoxicity of myeloid cell leukemia-1 siRNA versus scrambled siRNA micelles. The viability of the MDA-MB-435 after 72 h exposure to polymer/siRNA micelles prepared using the scrambled and MCL-1 siRNA at polymer:siRNA ratios of 16:1 (w/w). 50 nM indicate the dose of siRNA used in each well. The data are the mean ± standard error of the mean (n = 3).
*Significantly different from its corresponding scrambled siRNA group (unpaired Student's *t*-test, $p < 0.05$).
#Significantly lower than MCL-1 siRNA/PEO-*b*-P(CL-*g*-SP) group (unpaired Student's *t*-test, $p < 0.05$).
MCL-1: Myeloid cell leukemia-1; PEO-*b*-P(CL-*g*-SP): Poly(ethylene oxide)-*block*-poly(α-carboxylate-ε-caprolactone-*grafted*-spermine); w/w: Weight/weight.

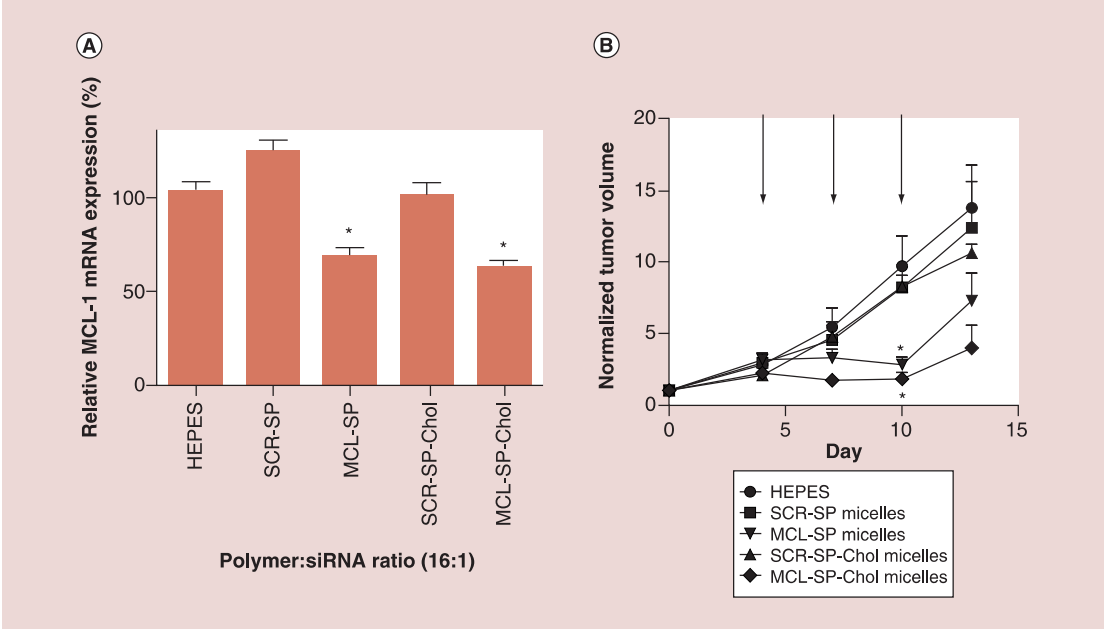

Figure 10. *In vivo* MCL-1 siRNA activity in nude mice-bearing MDA-MB-435 xenograft treated with three intratumoral injections of polymer/siRNA formulations or HEPES. (A) Relative MCL-1 mRNA expression in MDA-MB-435 xenograft after treatment with polymer/siRNA formulations or HEPES. Values are relative to untreated control. The data are presented as mean ± SEM (n = 4–5). *Significantly different from its corresponding scrambled siRNA group (one-way ANOVA followed by Tukey's *post hoc* test, $p < 0.05$). **(B)** Normalized tumor volume of MDA-MB-435 xenograft after treatment with polymer/siRNA formulations or HEPES. Each point represents mean ± SEM *(n = 4–5)*. Arrow indicates onset of intratumoral injection. *Significantly different from its corresponding scrambled siRNA group or HEPES (one-way ANOVA followed by Tukey's *post hoc* test, $p < 0.05$).
MCL-1: Myeloid cell leukemia-1; SEM: Standard error of the mean.

tumor growth when compared with control animals, however. This may be because the formulation does not have easy access to the core of the tumor and may be sequestered by tumor vasculature. Hence, higher MCL-1 mRNA downregulation (>40%) in the tumor cells might be required to see any measurable difference in inhibition of MDA-MB-435 tumor growth. Previous studies of *MCL-1* silencing in MDA-MB-435 have shown that PEI-LA complexes with 18 nM MCL-1 siRNA at siRNA:polymer ratios (w/w) of 1:8 were able to decrease the MCL-1 mRNA expression by approximately 80% and also reduced cell viability by up to approximately 50% *in vitro*. *In vivo* studies in MDA-MB-435 xenografts showed an approximately 35% decrease in MCL-1 mRNA expression and delayed tumor growth after intratumoral injections with PEI-LA/MCL-1 siRNA complexes, however, after intraperitoneal injections, MCL-1 mRNA expression decreased by approximately 20% but did not result in any significant tumor retardation [35].

The treatments did not have any adverse impact on the activity level and mean body weight of the animals. Also, histopathological examination of the kidney, spleen, and liver tissues did not show any toxicity confirming the safety of the siRNA and the selected delivery system in the mouse model employed. These results point to the relative safety of the siRNA complexes following intravenous injection.

Figure 11. *In vivo* MCL-1 siRNA activity in nude mice-bearing MDA-MB-435 xenograft treated with three intravenous injections of polymer/siRNA formulations or dextrose (see facing page). (A) Relative MCL-1 mRNA expression in MDA-MB-435 xenograft after treatment with polymer/siRNA formulations or dextrose. Values are relative to untreated control. The data are presented as mean ± SEM (n = 3–5). **(B)** Normalized tumor volume of MDA-MB-435 xenograft after treatment with polymer/siRNA formulations or dextrose. Each point represents mean ± SEM (n = 3–5). Arrow indicates onset of intravenous injection. **(C)** Percentage change in mean animal body weight after treatment with polymer/siRNA formulations or dextrose. Each point represents mean ± SEM (n = 3–5). *Significantly different from dextrose treated group (one-way ANOVA followed by Tukey's *post hoc* test, $p < 0.05$). **(D)** Microscopic histology images of the spleen, liver and kidney cortex stained with hematoxylin and eosin at 100×. Each image is representative of one mouse from a group of three.
MCL-1: Myeloid cell leukemia-1; SEM: Standard error of the mean.

A
Relative MCL-1 mRNA expression (%)
100
50
0
Dextrose
NON-SP
RGD-SP
NON-SP-Chol
RGD-SP-Chol
*
*
B
Normalized tumor volume
8
6
4
2
0
0
5
10
15
Days
Dextrose
NON-SP
RGD-SP
NON-SP-Chol
RGD-SP-Chol
C
Change in mean body weight (%)
20
15
10
5
0
-5
0
5
10
15
Days
Dextrose
NON-SP
RGD-SP
NON-SP-Chol
RGD-SP-Chol
D
Dextrose
NON-SP
RGD-SP
NON-SP-Chol
RGD-SP-Chol
Kidney
Liver
Spleen

Conclusion

In this study, we have reported the design, synthesis and evaluation of cholesteryl substitution on PEO-*b*-polyester-based polycationic copolymers, and explored its potential in silencing of *MCL-1* that is involved in cancer survival and progression. We demonstrated that cholesteryl substitution of PEO-*b*-P(CL-*g*-SP) improved the thermodynamic stability of PEO-*b*-P(CL-*g*-SP), and increased the cellular uptake of complexed siRNA by MDA-MB-435 cells. The increased delivery of MCL-1 siRNA into MDA-MB-435 cells translated into efficient downregulation of MCL-1 mRNA expression and subsequent inhibition of cell growth, *in vitro*. However, this trend was not observed following administration of the cholesterol-modified siRNA micellar complexes, *in vivo*, either following intratumoral or intravenous administration, where both PEO-*b*-P(CL-*g*-SP) and PEO-*b*-P(CL-*g*-SP-Chol) MCL-1 siRNA complexes showed significant but similar downregulation of MCL-1 mRNA expression (by 30–40%) after intratumoral administration. Following intravenous administration, *MCL-1* silencing in tumor achieved by unmodified SP- or SP-Chol siRNA complexes was around 10–20%. Surface modification of polymeric micellar siRNA with RGD4C increased the *MCL-1* silencing activity of both micellar complexes in tumor xenografts similarly (reaching around 40% silencing) after systemic administration. Our results also demonstrated the safety and potential of targeted PEO-*b*-P(CL-*g*-SP)-based micelles for gene silencing in tumor following localized or systemic siRNA administration.

Future perspective

Targeted delivery of RNA entities to different organs/cells has been of much interest during the past decade. Limited success has been achieved in delivery of RNA therapeutics to organs like liver in preclinical and clinical trials. But examples of successful targeted RNA delivery systems to solid tumors following systemic administration are infrequent. We have reported on a polymeric micellar delivery system with potential in achieving this goal, which is expected to be of tremendous interest. Further studies on the detailed characterization (e.g., for zeta potential and size in biomimetic media and safety profile at different doses *in vivo*), optimization (e.g., for more efficient and specific tumor cell transfection) and validation (e.g., for applicability in efficient delivery of siRNAs targeting other genes and other entities like mRNA) of this delivery system are ongoing in our research group.

Supplementary data

To view the supplementary data that accompany this paper please visit the journal website at: www.futuremedicine.com/doi/full/10.2217/nnm-2016-0178

Acknowledgements

The authors thank D McGinn, Department of Oncology, University of Alberta, for assistance with IV (tail-vein) injections; S Lamb, Department of Medical Microbiology and Immunology, University of Alberta, for assistance with tissue processing and slide preparation for histopathological studies; and PN Nation, Animal Pathology Services (APS) Ltd, for assistance with histopathological analysis.

Financial & competing interests disclosure

This study was supported by a grant from the Canadian Institute of health Research (CIHR) (MOP 137153). SM Garg was supported by the Alberta Innovates Health Solutions

Executive summary

- Poly(ethylene oxide)-*block*-poly(e-caprolactone-*grafted*-spermine) (PEO-*b*-P(CL-*g*-SP)) micelles were modified with hydrophobic cholesteryl groups in the core.
- PEO-*b*-P(CL-*g*-SP) and cholesteryl-modified PEO-*b*-P(CL-*g*-SP), that is, PEO-*b*-P(CL-*g*-SP-Chol) were modified with cancer-targeting peptide RGD4C at the shell.
- Cholesteryl modification of the core resulted in micelles having a smaller size and lower critical micelle concentration indicating improved assembly and/or stability.
- siRNA complexed with cholesteryl-modified PEO-*b*-P(CL-*g*-SP) micelles showed better cellular association and lower toxicity in MDA-MB-435 cancer cells, when compared with unmodified PEO-*b*-P(CL-*g*-SP).
- Higher cellular association of PEO-*b*-P(CL-*g*-SP-Chol) led to better silencing of *MCL-1* in MDA-MB-435 cells *in vitro*.
- Both PEO-*b*-P(CL-*g*-SP) and PEO-*b*-P(CL-*g*-SP-Chol) showed better *MCL-1* silencing and inhibition of tumor growth compared with control group following intratumoral administration in MDA-MB-435 subcutaneous xenograft.
- RGD4C modification of the micellar shell of both PEO-*b*-P(CL-*g*-SP) and PEO-*b*-P(CL-*g*-SP-Chol) led to higher *MCL-1* silencing when compared with control group following intravenous administration in MDA-MB-435 subcutaneous xenograft.
- Cholesteryl modification of the core did not significantly improve the silencing activity of MCL-1 siRNA when compared with unmodified PEO-*b*-P(CL-*g*-SP) after both, local and systemic administration.

(AIHS) Graduate Studentship, ACF Graduate Studentship and the JN Tata Trust Scholarship. A Falamarzian was supported by the ACF Graduate Studentship. The polymers developed and used for siRNA delivery in this research are licensed to Meros Polymers Inc. (University of Alberta, AB, Canada). The authors have no other relevant affiliations or financial involvement with any organization or entity with a financial interest in or financial conflict with the subject matter or materials discussed in the manuscript apart from those disclosed.

No writing assistance was utilized in the production of this manuscript.

Ethical conduct of research

The authors state that they have obtained appropriate institutional review board approval or have followed the principles outlined in the Declaration of Helsinki for all human or animal experimental investigations. In addition, for investigations involving human subjects, informed consent has been obtained from the participants involved.

References

Papers of special note have been highlighted as: • of interest; •• of considerable interest

1 Yu YH, Kim E, Park DE *et al.* Cationic solid lipid nanoparticles for co-delivery of paclitaxel and siRNA. *Eur. J. Pharm. Biopharm.* 80(2), 268–273 (2012).

2 Chang RS, Suh MS, Kim S *et al.* Cationic drug-derived nanoparticles for multifunctional delivery of anticancer siRNA. *Biomaterials* 32(36), 9785–9795 (2011).

3 Aliabadi hM, Mahdipoor P, Uludag h. Polymeric delivery of siRNA for dual silencing of Mcl-1 and P-glycoprotein and apoptosis induction in drug-resistant breast cancer cells. *Cancer Gene Ther.* 20(3), 169–177 (2013).

4 Leng Q, Woodle MC, Lu PY, Mixson AJ. Advances in systemic siRNA delivery. *Drugs Future* 34(9), 721 (2009).

5 Aliabadi hM, Mahmud A, Sharifabadi AD, Lavasanifar A. Micelles of methoxy poly(ethylene oxide)-b-poly(epsilon-caprolactone) as vehicles for the solubilization and controlled delivery of Cyclosporine A. *J. Control. Release* 104(2), 301–311 (2005).

6 Diao YY, Li hY, Fu YH *et al.* Doxorubicin-loaded PEG-PCL copolymer micelles enhance cytotoxicity and intracellular accumulation of doxorubicin in adriamycin-resistant tumor cells. *Int. J. Nanomedicine* 6, 1955–1962 (2011).

7 Zhang XC, Jackson JK, Burt hM. Development of amphiphilic diblock copolymers as micellar carriers of taxol. *Int. J. Pharm.* 132(1–2), 195–206 (1996).

8 Jeong B, Bae YH, Kim SW. Biodegradable thermosensitive micelles of PEG-PLGA-PEG triblock copolymers. *Colloid Surface B* 16(1–4), 185–193 (1999).

9 Yoo hS, Park TG. Biodegradable polymeric micelles composed of doxorubicin conjugated PLGA-PEG block copolymer. *J. Control. Release* 70(1–2), 63–70 (2001).

10 Xiong XB, Falamarzian A, Garg SM, Lavasanifar A. Engineering of amphiphilic block copolymers for polymeric micellar drug and gene delivery. *J. Control. Release* 155(2), 248–261 (2011).

11 Adams ML, Lavasanifar A, Kwon GS. Amphiphilic block copolymers for drug delivery. *J. Pharm. Sci.* 92(7), 1343–1355 (2003).

12 Yang L, El Ghzaoui A, Li S. *In vitro* degradation behavior of poly(lactide)-poly(ethylene glycol) block copolymer micelles in aqueous solution. *Int. J. Pharm.* 400(1–2), 96–103 (2010).

13 Xiong X-B, UludaĞ h, Lavasanifar A. Biodegradable amphiphilic poly(ethylene oxide)-block-polyesters with grafted polyamines as supramolecular nanocarriers for efficient siRNA delivery. *Biomaterials* 30(2), 242–253 (2009).

• **Reports on the design, synthesis and evaluation of a new family of poly(ethylene oxide)-*b*-polyester-based polycationic copolymers for siRNA delivery.**

14 Xiong XB, Uludag h, Lavasanifar A. Virus-mimetic polymeric micelles for targeted siRNA delivery. *Biomaterials* 31(22), 5886–5893 (2010).

15 Xiong XB, Lavasanifar A. Traceable multifunctional micellar nanocarriers for cancer-targeted co-delivery of MDR-1 siRNA and doxorubicin. *ACS Nano* 5(6), 5202–5213 (2011).

•• **Demonstrates the potential of multifunctional micellar nanomedicine for delivery of anticancer drugs and oncogene-silencing siRNA to their intended targets.**

16 Hsu CY, Uludag h. Cellular uptake pathways of lipid-modified cationic polymers in gene delivery to primary cells. *Biomaterials* 33(31), 7834–7848 (2012).

17 Falamarzian A, Aliabadi hM, Molavi O *et al.* Effective down-regulation of signal transducer and activator of transcription 3 (STAT3) by polyplexes of siRNA and lipid-substituted polyethyleneimine for sensitization of breast tumor cells to conventional chemotherapy. *J. Biomed. Mater. Res. A* 102(9), 3216–3228 (2014).

18 Furgeson DY, Chan WS, Yockman JW, Kim SW. Modified linear polyethylenimine-cholesterol conjugates for DNA complexation. *Bioconjug. Chem.* 14(4), 840–847 (2003).

19 Gusachenko Simonova O, Kravchuk Y, Konevets D, Silnikov V, Vlassov VV, Zenkova MA. Transfection efficiency of 25-kDa PEI-cholesterol conjugates with different levels of modification. *J. Biomater. Sci. Polym. Ed.* 20(7–8), 1091–1110 (2009).

20 Furgeson DY, Yockman JW, Janat mm, Kim SW. Tumor efficacy and biodistribution of linear polyethylenimine-cholesterol/DNA complexes. *Mol. Ther.* 9(6), 837–845 (2004).

21 Wang Y, Gao S, Ye WH, Yoon hS, Yang YY. Co-delivery of drugs and DNA from cationic core-shell nanoparticles self-assembled from a biodegradable copolymer. *Nat. Mater.* 5(10), 791–796 (2006).

22 Adams KW, Cooper GM. Rapid turnover of MCL-1 couples translation to cell survival and apoptosis. *J. Biol. Chem.* 282(9), 6192–6200 (2007).

23 Thomas LW, Lam C, Edwards SW. MCL-1; the molecular regulation of protein function. *FEBS Lett.* 584(14), 2981–2989 (2010).

24 Kozopas KM, Yang T, Buchan hL, Zhou P, Craig RW. MCL1, a gene expressed in programmed myeloid cell differentiation, has sequence similarity to BCL2. *Proc. Natl Acad. Sci. USA* 90(8), 3516–3520 (1993).

25 Le Gouill S, Podar K, Harousseau JL, Anderson KC. MCL-1 regulation and its role in multiple myeloma. *Cell Cycle (Georgetown, Tex.)* 3(10), 1259–1262 (2004).

26 Modugno M, Banfi P, Gasparri F *et al.* MCL-1 antagonism is a potential therapeutic strategy in a subset of solid cancers. *Exp. Cell Res.* 332(2), 267–277 (2014).

27 Ding Q, huo L, Yang JY *et al.* Down-regulation of myeloid cell leukemia-1 through inhibiting Erk/Pin 1 pathway by sorafenib facilitates chemosensitization in breast cancer. *Cancer Res.* 68(15), 6109–6117 (2008).

28 Akgul C. MCL-1 is a potential therapeutic target in multiple types of cancer. *Cell. Mol. Life Sci.* 66(8), 1326–1336 (2009).

• **Excellent review summarizing the current strategies in regulation of MCL-1 expression and new approaches for targeting MCL-1 in cancer cells.**

29 Mitchell C, Yacoub A, hossein h *et al.* Inhibition of MCL-1 in breast cancer cells promotes cell death *in vitro* and *in vivo*. *Cancer Biol. Ther.* 10(9), 903–917 (2010).

30 Jazirehi AR, Bonavida B. Resveratrol modifies the expression of apoptotic regulatory proteins and sensitizes non-Hodgkin's lymphoma and multiple myeloma cell lines to paclitaxel-induced apoptosis. *Mol. Cancer Ther.* 3(1), 71–84 (2004).

31 Nguyen M, Marcellus RC, Roulston A *et al.* Small molecule obatoclax (GX15–070) antagonizes MCL-1 and overcomes MCL-1-mediated resistance to apoptosis. *Proc. Natl Acad. Sci. USA* 104(49), 19512–19517 (2007).

32 Lee EF, Czabotar PE, Van Delft MF *et al.* A novel BH3 ligand that selectively targets MCL-1 reveals that apoptosis can proceed without MCL-1 degradation. *J. Cell Biol.* 180(2), 341–355 (2008).

33 Aichberger KJ, Mayerhofer M, Gleixner KV *et al.* Identification of MCL1 as a novel target in neoplastic mast cells in systemic mastocytosis: inhibition of mast cell survival by MCL1 antisense oligonucleotides and synergism with PKC412. *Blood* 109(7), 3031–3041 (2007).

34 Chetoui N, Sylla K, Gagnon-Houde JV *et al.* Down-regulation of MCL-1 by small interfering RNA sensitizes resistant melanoma cells to FAS-mediated apoptosis. *Mol. Cancer Res.* 6(1), 42–52 (2008).

35 Aliabadi hM, Maranchuk R, Kucharski C, Mahdipoor P, Hugh J, Uludag H. Effective response of doxorubicin-sensitive and -resistant breast cancer cells to combinational siRNA therapy. *J. Control. Release* 172(1), 219–228 (2013).

36 Mahmud A, Xiong X, Lavasanifar A. Novel self-associating poly(ethylene oxide)-*block*-(ε-caprolactone) block copolymers with functional side groups on the polyester block for drug delivery. *Macromolecules* 39(26), 9419–9428 (2006).

•• **Reports on a novel family of poly(ethylene oxide)-*b*-polyester block copolymers having functional side groups, which can be exploited for the chemical conjugation, optimized solubilization, and controlled delivery of several therapeutic agents.**

37 Nikouei NS, Vakili MR, Bahniuk MS *et al.* Thermoreversible hydrogels based on triblock copolymers of poly(ethylene glycol) and carboxyl functionalized poly(epsilon-caprolactone): the effect of carboxyl group substitution on the transition temperature and biocompatibility in plasma. *Acta Biomater.* 12, 81–92 (2015).

38 Xiong XB, Mahmud A, Uludag h, Lavasanifar A. Multifunctional polymeric micelles for enhanced intracellular delivery of doxorubicin to metastatic cancer cells. *Pharm. Res.* 25(11), 2555–2566 (2008).

39 Xiong XB, Ma Z, Lai R, Lavasanifar A. The therapeutic response to multifunctional polymeric nano-conjugates in the targeted cellular and subcellular delivery of doxorubicin. *Biomaterials* 31(4), 757–768 (2010).

40 Zhao CL, Winnik MA, Riess G, Croucher MD. Fluorescence probe techniques used to study micelle formation in water-soluble block copolymers. *Langmuir* 6(2), 514–516 (1990).

41 Aliabadi hM, Landry B, Bahadur RK, Neamnark A, Suwantong O, Uludag H. Impact of lipid substitution on assembly and delivery of siRNA by cationic polymers. *Macromol. Biosci.* 11(5), 662–672 (2011).

42 Mosmann T. Rapid colorimetric assay for cellular growth and survival: application to proliferation and cytotoxicity assays. *J. Immunol. Methods* 65(1–2), 55–63 (1983).

43 Shahin M, Soudy R, Aliabadi HM, Kneteman N, Kaur K, Lavasanifar A. Engineered breast tumor targeting peptide ligand modified liposomal doxorubicin and the effect of peptide density on anticancer activity. *Biomaterials* 34(16), 4089–4097 (2013).

44 Akhtar S, Benter I. Toxicogenomics of non-viral drug delivery systems for RNAi: potential impact on siRNA-mediated gene silencing activity and specificity. *Adv Drug Deliv Rev* 59(2–3), 164–182 (2007).

45 Nishiyama N, Kataoka K. Nanostructured devices based on block copolymer assemblies for drug delivery: designing structures for enhanced drug function. In: *Polymer Therapeutics II* Satchi-Fainaro R, Duncan R (Eds). Springer Berlin, Heidelberg, 67–101 (2006).

46 Falamarzian A, Lavasanifar A. Chemical modification of hydrophobic block in poly(ethylene oxide) poly(caprolactone) based nanocarriers: effect on the solubilization and hemolytic activity of amphotericin B. *Macromol. Biosci.* 10(6), 648–656 (2010).

47 Zhang L, Khougaz K, Moffitt M, Eisenberg A. Self-Assembly of block polyelectrolytes. In: *Amphiphilic Block Copolymers.* Lindman PA (Ed.).Elsevier Science B.V., Amsterdam, The Netherlands, 87–113 (2000).

48 Khougaz K, Astafieva I, Eisenberg A. Micellization in block polyelectrolyte solutions. 3. Static light scattering characterization. *Macromolecules* 28(21), 7135–7147 (1995).

49 Mathews AS, Ahmed S, Shahin M, Lavasanifar A, Kaur K. Peptide modified polymeric micelles specific for breast cancer cells. *Bioconjug. Chem.* 24(4), 560–570 (2013).

50 Yamamoto Y, Nagasaki Y, Kato M, Kataoka K. Surface charge modulation of poly(ethylene glycol)–poly(d,l-lactide) block copolymer micelles: conjugation of charged peptides. *Colloids Surf. B. Biointerfaces* 16(1–4), 135–146 (1999).

51 Verma A, Stellacci F. Effect of surface properties on nanoparticle–cell interactions. *Small* 6(1), 12–21 (2010).

52 Frohlich E. The role of surface charge in cellular uptake and cytotoxicity of medical nanoparticles. *Int. J. Nanomedicine* 7, 5577–5591 (2012).

53 Chen K, Chen X. Integrin targeted delivery of chemotherapeutics. *Theranostics* 1 189–200 (2011).

54 Arap W, Pasqualini R, Ruoslahti E. Cancer treatment by targeted drug delivery to tumor vasculature in a mouse model. *Science* 279(5349), 377–380 (1998).

55 Wang h, Chen K, Cai W *et al.* Integrin-targeted imaging and therapy with RGD4C-TNF fusion protein. *Mol. Cancer Ther.* 7(5), 1044–1053 (2008).